

Vibrations of the *p*-chlorofluorobenzene cation

David J. Kemp, Laura E. Whalley, William D. Tuttle, Adrian M. Gardner, Benjamin T. Speake, and Timothy G. Wright*

School of Chemistry, University of Nottingham, University Park, Nottingham, NG7 2RD, U.K.

*To whom correspondence should be addressed. Email: Tim.Wright@nottingham.ac.uk

Abstract

The vibrations of the ground state cation (\tilde{X}^2B_1) of *para*-chlorofluorobenzene (*p*CIFB) have been investigated using zero-electron-kinetic-energy (ZEKE) spectroscopy. ZEKE spectra were recorded using different vibrational levels of the S_1 state as intermediate levels, for which assignments were put forward in an earlier paper [W. D. Tuttle, A. M. Gardner, and T. G. Wright, Chem. Phys. Lett. **684**, 339 (2017)]. These different intermediate levels dramatically modify the Franck-Condon factors for the ionization step. The adiabatic ionization energy (AIE) for *p*CIFB was measured as 72919 ± 5 cm⁻¹, and analysis of the vibrational structure in the ZEKE spectra allowed further interrogation of the assignments of the REMPI spectrum. Assignment of the vibrational structure has been achieved by comparison with corresponding spectra of related molecules, via quantum chemical calculations, and via shifts in bands between the spectra of the ³⁵Cl and ³⁷Cl isotopologues. In this way it was possible to assign twenty out of the thirty vibrational modes of the ground state *p*CIFB⁺ cation. Additionally, evidence for Fermi resonances between some vibrational levels was found, but no large-scale intramolecular vibrational redistribution (IVR) was seen in the spectra here. Finally, we discuss trends in AIE shifts for benzenes with one or two halogen atoms or methyl substituents.

Introduction

In recent work from our group, we have focused on the study of vibrations of substituted benzenes in the S_1 state and cation, with a particular interest in identifying common activity across related molecular species. We have recorded resonance-enhanced multiphoton ionization (REMPI) spectra of the three lightest monohalobenzenes,^{1,2,3} toluene^{4,5}, *para*-fluorotoluene (*p*FT)^{6,7,8} and *para*-xylene (*p*Xyl)^{9,10}. The establishment of common activity across a series of molecules requires the use of a consistent labelling scheme, which we have noted is required to be different for monosubstituted benzenes,¹¹ *ortho*-¹² *meta*-¹³ and the *para*-disubstituted benzenes.¹⁴ We shall employ the latter scheme in the present work.

Very recently, we reported the REMPI spectrum of *para*-chlorofluorobenzene (*p*CIFB)¹⁵ where we made assignments based on expected activity and quantum chemical calculation of the harmonic vibrational wavenumbers, together with shifts for the $p^{35}\text{CIFB}$ and $p^{37}\text{CIFB}$ isotopologues. We have now completed a study of the corresponding cation, employing zero-electron-kinetic-energy (ZEKE) (photoelectron) spectroscopy, which we have recorded *via* different intermediate S_1 vibrational levels.

As noted in our earlier work,¹⁵ there appear to be only a few studies on the spectroscopy of *p*CIFB, with the available S_0 vibrational wavenumbers having been discussed in Ref. 14 (see also, Refs. 16 and 17). With regards to the S_1 state, the origin transition was analysed via UV absorption spectroscopy by Cvitaš and Hollas.¹⁸ Pertinent to the present study would seem to be a REMPI study from Numata et al.,¹⁹ but although the authors reported a number of band positions, no assignments were made. In passing, we note that there has also been a REMPI study of the *p*CIFB-methanol complex by Riehn et al.,²⁰ but the corresponding spectrum of the monomer was not presented.

Finally, we note that the adiabatic ionization energy (AIE) of *p*CIFB has been determined by a number of workers, with three employing conventional photoelectron spectroscopy (PES).^{21,22,23} None of the spectra in these studies showed clear vibrational structure for the \tilde{X}^2B_1 state, nor was there any such in an emission study of the cation.²⁴ The most precise value for the AIE appears to be that of Lias and Ausloos²⁵ who employed mass spectrometric charge transfer equilibrium measurements to establish the heats of formation and consequently AIEs of a wide set of organic compounds, with a value for *p*CIFB of 9.011 ± 0.008 eV being reported.

Experimental

The vapour above room temperature *para*-chlorofluorobenzene (98% purity, Aldrich) was seeded in ~1.5 bar of Ar and the gaseous mixture passed through a General Valve pulsed nozzle (750 μm , 10 Hz, opening time of ~200 μs) to create the free jet expansion. The focused, frequency-doubled outputs of two dye lasers were overlapped spatially and temporally and passed through a vacuum chamber coaxially and counterpropagating, where they intersected the free jet expansion between two biased electrical grids. These were located in the extraction region of a time-of-flight mass spectrometer, which was employed in the REMPI experiments. These grids were also used in the ZEKE experiments by application of pulsed voltages, after a delay of up to 2 μs , giving typical fields (F) of ~10 V cm^{-1} . This delay was minimized while avoiding contributions from the prompt electron signal. The resulting ZEKE bands had widths of ~5-7 cm^{-1} . The ionization laser was a dye laser (Sirah Cobra-Stretch) operating with C540A, and pumped with the third harmonic (355 nm) of a Surelite III Nd:YAG laser. The excitation laser was a dye laser (Sirah Cobra-Stretch) operating also with C540A, and pumped with the third harmonic (355 nm) of a Surelite I Nd:YAG laser. The fundamental outputs produced by each dye laser were frequency doubled using BBO crystals for the pump and probe lasers, respectively. The REMPI spectra were recorded in the parent mass channel, with separate spectra recorded for the ^{35}Cl and ^{37}Cl isotopologues. They were recorded as two-colour spectra, with the ionizing photon being 37990 cm^{-1} , as it is not possible to ionize via the $S_1 \leftarrow S_0$ transition in a (1+1) REMPI process in the first ~ 350 cm^{-1} . (For convenience we continued with the two-colour scheme for the range of the spectrum shown.) Calibration of the REMPI spectrum has been achieved by setting the origin band position to that of Cvitaš and Hollas,¹⁸ with the uncertainty estimated from the width of the rotational profile. The calibration of the ionization laser could be checked against “accidental resonance” electron signals, which originate from $S_1 \leftarrow S_0$ transitions; these will be discussed further below.

Calculational details

We have employed the B3LYP density functional theory method, which we and others have shown is reliable for calculating vibrational wavenumbers for the ground state cation, D_0^+ of substituted benzenes. For the S_1 states, we have utilized the time-dependent B3LYP (TD-B3LYP) method, as in previous work, but its performance is more variable (see below). The

basis sets employed are aug-cc-pVTZ, which we have also used in previous work. The Gaussian package²⁶ was used for all calculations reported herein. We note that all calculated wavenumbers have been scaled by 0.97 to correct both for anharmonicity and other weaknesses in the method. Additionally, as we have commented on previously,^{3,6,9} the lowest wavenumber a_2 vibration (D_{14} here) of the S_1 state does not appear to be described well for substituted benzenes (note that the molecule lies in the yz plane) and we do not report values for this vibration, instead relying on the appearance of the spectrum to assign transitions involving this vibration. It is unclear what the cause is for the unreliability of this calculated value, but we are undertaking a study of this using different functionals and other quantum chemical approaches. Although not as stark, there are also issues with the calculation of the other out-of-plane modes (a_2 and b_1 symmetry) in the S_1 state, and we discussed these in Ref. 15, where the wavenumbers of all but one of the out-of-plane modes of the S_1 state were established experimentally. On the other hand, the calculated values of the in-plane modes (a_1 and b_2 symmetry) were generally reliable. These issues do not affect the calculated vibrational wavenumbers of the D_0^+ state, and hence we expect the wavenumbers of bands in the ZEKE spectrum to be predicted well by the calculated values, and this will allow testing of the previous S_1 state vibrational assignments.¹⁵

We present calculated vibrational wavenumbers for $p^{35}\text{ClFB}$ in Table 1 for both the S_1 and D_0^+ states; in addition, we present the calculated $^{35}\text{Cl}/^{37}\text{Cl}$ isotopic shift for each vibration.

Results and Discussion

REMPI spectrum

In Figure 1(a) we show an overview of the REMPI spectra of $p^{35}\text{ClFB}$ up to $\sim 1400\text{ cm}^{-1}$. Excitations are almost exclusively from the zero-point vibrational level in the S_0 state, and this lower level is omitted when specifying transitions. The origin of the $S_1 \leftarrow S_0$ transition has been established as $36275 \pm 2\text{ cm}^{-1}$,^{15,18} and is the same for both isotopologues, within 1 cm^{-1} as judged from the position and band profiles. This spectrum has been presented in Ref. 15, and its assignment discussed therein on the basis of quantum chemical calculations, isotopic shifts in some bands, and by comparison with similar molecules. In almost all cases, the bands for $p^{35}\text{ClFB}$ and $p^{37}\text{ClFB}$ overlap, and so contributions from both isotopologues will be present in

the ZEKE spectra. Even in the few cases where the shifts are discernible, the REMPI band profiles from both isotopologues are still partially overlapped, and so the ZEKE bands will still generally arise from both isotopologues, but to varying extents. The main activity in the REMPI spectrum is associated with Franck-Condon (FC) activity in a_1 symmetry modes, including fundamentals, overtones and combinations, but also Herzberg-Teller (HT) vibronically-induced bands of b_2 symmetry are observed.

ZEKE Spectra

ZEKE spectrum via $S_1 0^0$

In Figure 2(a) we show the ZEKE spectrum of *p*CIFB recorded via the $S_1 0^0 \leftarrow S_0$ transition. As may be seen, it consists of a very strong band at the origin, consistent with the expected $\Delta v = 0$ propensity rule, with a number of other bands to higher wavenumber. The first band can be associated with the adiabatic ionization energy (AIE) and the sum of the wavenumbers of the excitation and ionization lasers then allows the AIE to be derived as $72919 \pm 5 \text{ cm}^{-1}$ ($9.0408 \pm 0.0006 \text{ eV}$). This value agrees fairly well with the value from Lias and Ausloos²⁵ of $9.011 \pm 0.008 \text{ eV}$ ($72680 \pm 60 \text{ cm}^{-1}$), but the present value is clearly somewhat higher, with the latter perhaps affected by thermal effects. The ZEKE features to higher wavenumber in Figure 2(a) can be associated with vibrational activity in the cation, and the assignments are based upon the calculated cation wavenumbers in Table 1, and confirmed by activity in other ZEKE spectra discussed below. We note that we expect the main ZEKE structure to arise from FC activity in a_1 symmetry modes, including fundamentals, overtones and combinations, but also HT vibronically-induced bands of b_1 and a_2 symmetry, and possibly b_2 symmetry. With these points in mind, the assignments of the spectrum can be achieved, as indicated in Figure 2(a), with the 11^1 , 9^1 , 8^1 and 7^1 bands being straightforwardly identified. To low wavenumber we see bands from transitions to two b_1 symmetry modes, 20^1 and 19^1 , as well as to the a_2 mode 14^1 . The 19^1 and 14^1 bands are common in the ZEKE spectra of *para*-disubstituted benzenes^{4,6,9,10} and appear to arise from vibronic coupling in the cation; the 20^1 transition has also been observed in *p*FT⁶ and *p*Xyl⁹ although in those cases vibration-torsion (vibtor) levels have to be considered. Above the 11^1 feature, a number of weak non-FC bands are seen, with the 28^1 notable as it is of b_2 symmetry; again, this is likely vibronically induced – see Ref. 6 for further discussion on vibronic coupling in substituted benzene cations. Other bands are then

relatively straightforward to assign, and the assignments can be cross-checked against those of other spectra reported in the present work, to ensure internal consistency with the derived wavenumbers for the fundamentals, and also expected good agreement with the calculated wavenumbers. The derived wavenumbers are reported in Table 1.

“Accidental Resonances”

In recording the ZEKE spectra, it quickly became apparent that some very narrow bands appeared, which do not arise from the standard (1+1') ZEKE process. These signals could be quite intense and, frustratingly, quite often severely overlapped a ZEKE band. They are indicated in the spectra, such as in Figure 2(a), by an asterisk or a dagger (†), as there are two distinct routes for their formation, each facilitated by the fact that the S_1 state lies half-way between the S_0 state and the ground state cation, D_0^+ , state.

The first route is via two-photon, one-colour resonant ionization and an example trace is seen in Figure 1(b). It will be noticed that the positions of these accidental resonances are coincident with REMPI bands, but the intensities are different. They arise since a second photon from the excitation laser takes the resonant S_1 state to a resonant or quasi-resonant level in the cation. An “accidental resonance” signal will be produced if the two-photon energy takes the molecule to high-lying Rydberg states just below an ionization threshold, which are then ionized by the pulsed-field extraction, in the usual way for ZEKE spectroscopy. (Such a signal could also arise when the two-photon energy is just above threshold, if the number of ions present at the laser focus is sufficient to “trap” these slow electrons.) In both cases, we expect a narrow band, since the production of the Rydberg states (or slow electrons) can only occur across a narrow wavenumber range when the laser is resonant with a $S_1 \leftarrow S_0$ transition. These one-colour accidental resonance signals appear across the ZEKE spectra, and are labelled with an asterisk in each case.

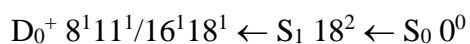
Such spurious signals were seen in earlier work on *para*-difluorobenzene (*p*DFB) by Müller-Dethlefs and coworkers.^{27,28} In that work, they attributed the signals to electrons produced in a REMPI process. As the ionization laser is scanned, it is occasionally resonant with an $S_1 \leftarrow S_0$ transition, and when this occurs, a large increase in one-colour resonant ionization occurs and this produces a large number of ions and electrons. It was suggested that the spurious electron

signals arose as the result of trapping those electrons in the ion cloud, which then survived the time delay until the pulsed electric field extraction occurs and so the signal appeared in the same time gate as the ZEKE electrons. This occurs in *p*DFB because the S_1 state is located half-way between the S_0 and D_0^+ states. A similar situation occurs in *p*CIFB, but as we have noted, we believe the explanation is a little more subtle, since we do not see all REMPI transitions appearing in the “accidental resonance” scan – compare Figures 1(a) and 1(b).

To give an example, we take the most intense feature in the accidental resonance electron spectrum, which may be seen from Figure 1(b) to be resonant with the $S_1 29^1 \leftarrow S_0 0^0$ transition. We also find that this photon wavenumber is coincidentally resonant with the $D_0^+ 29^1 \leftarrow S_1 29^1$ transition, and so gives rise to a signal in the ZEKE gate following one-colour, two-photon ($1 + 1$) absorption, as described above. This can be seen in Figure 2(b), where we have shown the two-photon, one-colour accidental resonance signals on a relative wavenumber scale that matches that of the ZEKE spectrum; comparison of Figures 1 and 2 emphasise the fact that an accidental resonance occurs in *both* the S_1 and D_0^+ states. The other accidental resonance electron transitions may be deduced from Figures 1 and 2 to be:



and



It is interesting to note that the first transition involves b_2 symmetry levels, and retains the vibrational excitation, i.e. is a $\Delta v = 0$ transition, perhaps explaining why its intensity is the greatest. Similarly, the second case involves an S_1 level that arises from a Fermi resonance involving the overtone of D_{29} , and then the second resonant transition is to $11^1 29^2$, also expected to have a reasonable Franck-Condon factor (FCF). In the final case, there are two D_0^+ levels that are very close in wavenumber and both are of a_1 symmetry and both might be expected to have reasonable FCFs from the $S_1 18^2$ level, $16^1 18^1$ and $8^1 11^1$, although the $16^1 18^1$ looks slightly more attractive based on quantum number changes.

A second, but related, mechanism also occurs that depends on both laser wavenumbers – i.e. it is a two-colour process. In these cases, the scanning “ionization” laser in the ZEKE experiment becomes resonant with the energy of an $S_1 \leftarrow S_0$ transition and, additionally, the fixed “excitation” laser is then resonant with a transition from this S_1 level, to a level in the cation.

This then leads to the production of either high-lying Rydberg states (or perhaps very slow electrons), as noted above. These signals are labelled with a dagger (†) in the ZEKE spectra and will be discussed as they arise in the spectra.

In both cases, it is relatively straightforward to identify the “accidental resonance” bands in the ZEKE spectra, because of their narrowness, and then to assign them on the basis of the laser wavenumbers, as discussed.

ZEKE spectra via $S_1 20^2$, 19^2 and 18^2

The three ZEKE spectra recorded when excited through the overtones of three vibrations each of b_1 symmetry are shown in Figure 3. These S_1 vibrational levels are of overall a_1 symmetry, and the REMPI bands are consistent with activity in the $S_1 \leftarrow S_0$ excitation spectra of *para*-disubstituted benzenes,^{6,9,29} with the assignment of these discussed in more detail in Ref. 15.

The ZEKE spectrum via $S_1 20^2$ in Figure 3(a) shows a strong $\Delta v = 0$ band at 204 cm^{-1} , which gives a value for D_{20} in the cation of 102 cm^{-1} , and this is consistent with the weak band at this wavenumber in the ZEKE spectrum recorded via the origin – see Figure 2(a). To higher wavenumber we see a clear feature that is broader than the $\Delta v = 0$ band; this, and its wavenumber, confirm it as the $11^1 20^2$ transition, with the breadth arising from contributions from both ^{35}Cl and ^{37}Cl isotopologues. Transitions for these are overlapping in the $S_1 \leftarrow S_0$ transition, and this broadening is a clear signature of a ZEKE band arising from a vibration that involves D_{11} , since this vibration has the largest isotopic shift (see Table 1).

The ZEKE spectrum via $S_1 19^2$ in Figure 3(b) shows a clear $\Delta v = 0$ band at 554 cm^{-1} , which establishes a value for D_{19} in the cation of 277 cm^{-1} , and again this is consistent with the appearance of the weak 19^1 band seen when exciting via the origin. To higher wavenumber a weak, broad feature is seen that is straightforwardly assigned as $11^1 19^2$.

Finally, for the last of these three overtone bands, the ZEKE spectrum via $S_1 18^2$ in Figure 3(c) shows a rather unusual spectrum in that there is no dominant $\Delta v = 0$ band. The calculated wavenumber for the cation D_{18} , and evidence from other spectra, support the most intense

ZEKE band at 1008 cm^{-1} as being due to 18^2 , giving an experimental value for D_{18} in the cation of 504 cm^{-1} . The next intense band at 984 cm^{-1} is straightforwardly assigned to 8^1 while the band at 962 cm^{-1} appears likely to be 16^120^1 , giving a D_{16} value in the cation consistent with the calculated value and also with bands assigned in other spectra. Neither of the latter two assignments are consistent with arising from a resonant $S_1 \leftarrow S_0$ overlapped transition. Hence, since these are of the same symmetry as the intermediate $2D_{18}$ level, these likely arise from FC activity or Duschinsky rotation of the corresponding vibrational coordinates between S_1 and D_0^+ . (We can rule out Fermi resonance in the cation since when exciting via 8^1 , we do not see the 18^2 ZEKE band – see later.) We note that the 16^120^1 transition arises from a combination of two out-of-plane b_1 symmetry modes, and the 18^2 band itself is an overtone of an out-of-plane b_1 symmetry mode, which is a possible rationale for this induced activity. We also see the 5^1 band at 1335 cm^{-1} . The value for D_{16} in the cation is consistent with the band at 1726 cm^{-1} arising from 16^2 – a not unexpected band given the 18^2 intermediate transition.

To lower wavenumber, the weak band at 579 cm^{-1} is tentatively assigned to 28^1 as this band is at the correct wavenumber, but its b_2 symmetry makes it surprising that this is seen, albeit weakly; another b_2 symmetry band is the weak band at 1632 cm^{-1} , assigned as 13^116^1 , which is consistent with the calculated values in Table 1. The band at 609 cm^{-1} can be assigned to 18^120^1 , which is consistent with the observation of 16^120^1 , noted above.

Lastly, we note that as well as one of the one-colour accidental resonances discussed above (which is overlapped by a possible two-colour accidental resonance, as well as the 8^111^1 ZEKE band) a further weak accidental resonance feature appears to high wavenumber at $\sim 1560\text{ cm}^{-1}$, marked with a dagger (\dagger). At this position, the “ionization” laser is resonant with the $S_16^1 \leftarrow S_0$ transition, and the “excitation” laser then resonantly ionizes to the $D_0^+ 13^2$ level.

ZEKE spectra via 30^1 , 29^1 and 28^1

In Figure 4 we show three ZEKE spectra, each recorded via an intermediate S_1 vibrational level of b_2 symmetry. These levels are active in the $S_1 \leftarrow S_0$ transition via HT vibronic coupling. We first consider the ZEKE spectrum obtained when exciting via the 30^1 intermediate level, shown in Figure 4(a). This shows a $\Delta v = 0$ band at 280 cm^{-1} consistent with being assigned to D_{30} in

the cation, in good agreement with the calculated value in Table 1. In addition, in each case we see a feature to higher wavenumber consistent with an assignment to 11^130^1 .

When exciting via the $S_1 29^1$ intermediate resonance, we see a $\Delta\nu = 0$ band at 421 cm^{-1} in the ZEKE spectrum in Figure 4(b), establishing the value for D_{29} in the cation; we also see the expected band assignable to 11^129^1 . Interestingly we also see the symmetry-allowed band corresponding to 11^130^1 , and although we might also have expected to see a band corresponding to 30^1 , this is outside the range of the scanned spectrum.

In this spectrum we note that the intensity of the “accidental resonance” band at just over 800 cm^{-1} is much more intense than expected – cf. Figure 1(b). The explanation for this is that at this wavenumber, the ionization laser becomes resonant with the $S_1 29^2 \leftarrow S_0$ transition, but also the “excitation laser” wavenumber is accidentally resonant with the $D_0^+ 11^129^2 \leftarrow S_1 29^2 \dots 9^1$ ionization transition. Hence either the “ionization” or “excitation” lasers can excite or ionize, leading to the enhanced intensity for this “spurious” band.

Further, we see another accidental resonance band at $\sim 575 \text{ cm}^{-1}$ in the ZEKE spectrum, marked with a dagger (\dagger). At this wavenumber, the “ionization” laser matches the $S_1 28^1 \leftarrow S_0$ transition, the “excitation” laser then ionizes to the $D_0^+ 28^1$ level in a $\Delta\nu = 0$ process.

Finally we recorded a ZEKE spectrum via 28^1 , shown in Figure 4(c), which demonstrates a clear $\Delta\nu = 0$ band at 581 cm^{-1} , confirming the wavenumber for D_{28} in the cation, and also a band to higher wavenumber consistent with 11^128^1 . The activity of 11^130^1 in the ZEKE spectrum recorded via 29^1 contrasts with the straightforward appearance of the spectra recorded via 30^1 and 28^1 , and may suggest small changes in the motion of the D_{29} vibration between the S_1 state and the cation.

ZEKE Spectra of $p\text{ClFB}$ via the $14^2/11^1$ bands

In Ref. 15 we deduced that the 14^2 and the 11^1 bands lay very close to each other for $p^{35}\text{ClFB}$ and were essentially coincident for $p^{37}\text{ClFB}$ – see the REMPI spectrum in the top trace in Figure 5. This behaviour was consistent with the D_{11} wavenumber shifting by $\sim 5 \text{ cm}^{-1}$ to lower

wavenumber for the heavier isotopologue, while the $2D_{14}$ overtone shifted by $\sim 1 \text{ cm}^{-1}$ so that both bands were essentially perfectly overlapped for the heavier isotopologue. In the lower part of Figure 5, we show ZEKE spectra recorded at three positions indicated in the REMPI spectrum. Based on the previous assignments,¹⁵ the ZEKE spectra should correspond to the following. Position A: the centre of the band corresponding to overlapped 14^2 and $11^1 p^{37}\text{ClFB}$ bands. Position B: maximum overlap between the $p^{35}\text{ClFB } 14^2$ band and the overlapped bands of $p^{37}\text{ClFB}$. Position C: the centre of the band corresponding to the 11^1 transition for $p^{35}\text{ClFB}$. The interpretation of the ZEKE spectra is less straightforward than would be hoped for, because of overlaps with the strong accidental resonance signals in this region. However, one can clearly identify the 14^2 band at 715 cm^{-1} on the basis of its wavenumber compared to the calculated value, and the assignment in the ZEKE spectrum recorded via the origin (see above); the band at 357 cm^{-1} is assigned as arising from 14^1 . These latter bands are extremely weak when exciting at Position C, as expected, with the observed activity likely due to HT activity. We do not think Fermi resonance is present, since the 11^1 and 14^2 bands are overlapped for $p^{37}\text{ClFB}$ and so not interacting to any great extent, which would have caused them to move apart in the REMPI spectrum.

Unfortunately, the bands arising from 11^1 are almost coincident with the accidental resonance band, and so cannot easily be discerned (see Figure 5). However, we can see the 11^2 bands to higher wavenumber. These seem consistent with seeing a single band at 759 cm^{-1} when exciting via the centre of the 11^1 transition for $p^{35}\text{ClFB}$ (Position C), while we see a single band at 749 cm^{-1} when exciting at the centre of the $11^1/14^2$ overlapped feature for $p^{37}\text{ClFB}$ (Position A). When exciting at Position B, signals are seen for both isotopologues of these in that ZEKE spectrum, from FC activity. Thus, the ZEKE spectra confirm the assignments of these REMPI features in Ref. 15. To higher wavenumber, other bands may be seen, most of whose assignment can be deduced from wavenumbers already established. These are indicated on the spectra in Figure 5.

Finally, we note that we did attempt to record a spectrum at the position of the weak REMPI band at $\sim 337 \text{ cm}^{-1}$, see Figure 5, which is assigned as $19^1 20^1$ in Ref. 15. The resulting ZEKE spectrum was weak and no band could be seen that was separate from the accidental resonances. (A ZEKE band would be expected at $\sim 379 \text{ cm}^{-1}$.) Neither was such a band discernible when exciting via the 11^1 or 14^2 intermediate levels. We are still comfortable with

this assignment, however, but we cannot make any definitive comment on whether the $D_{19}D_{20}$ level is interacting with D_{11} or $2D_{14}$ levels (i.e. FR), and so stealing intensity, or whether it is inherently bright.

In summary, although the accidental resonance electron signals are problematic, we are able to unpick and confirm the assignments of the main REMPI bands here, with the aid of ZEKE spectra via different intermediate levels and by reference to overtones in the ZEKE spectra that are unaffected by these signals.

ZEKE spectra recorded via 15^120^1 and 17^119^1

In their LIF study on *p*DFB, Knight and Kable²⁹ identified a number of combination bands that were composed of two b_1 symmetry vibrations, and so of overall a_1 symmetry. We were also able to identify a significant number of such bands in our REMPI and ZEKE study of *p*FT.^{6,7} Based on this, we assigned a number of bands in the REMPI spectrum of *p*CIFB to such combinations,¹⁵ where assignments in terms of fundamentals or overtones could not be found. In principle, these assignments can be tested by recording ZEKE spectra using those bands as intermediates; the spectra are usually quite definitive since shifts in b_1 vibrations upon ionization are usually substantial (see Table 1).

We note first that we were unsuccessful in recording ZEKE spectra via the bands assigned¹⁵ as 16^120^1 and 13^114^1 owing to their very low intensity – see Figure 1(a). We were, however, successful with recording ZEKE spectra via the 17^119^1 and 15^120^1 bands, which are shown in Figure 6. The first of these is quite simple, with only the $\Delta\nu = 0$ band seen alongside the accidental resonance electron features. Since we have already established the wavenumber of D_{19} , this allows the value of D_{17} in the cation to be established as 718 cm^{-1} , which is in good agreement with the calculated value (see Table 1); this assignment also confirms the corresponding S_1 value in Table 1. The spectrum via 15^120^1 has more structure in it. The calculated values help to establish that the $\Delta\nu = 0$ band is at 1088 cm^{-1} , and allows a value for D_{15} in the cation to be established as 987 cm^{-1} , in good agreement with the calculated value (see Table 1). Some of the other assignments are straightforward, using the criterion that they are likely to be totally symmetric, and based on wavenumber values already established. Two bands are worthy of comment. First, the only reasonable assignment for the band at 996 cm^{-1}

appears to be $17^1 19^1$. We considered whether the $D_{17}D_{19}$ and $D_{15}D_{20}$ levels might be in Fermi resonance – however, a $15^1 20^1$ band could not be seen in the ZEKE spectrum via $17^1 19^1$ although this was a significantly weaker REMPI band, and so it is possible such a band was simply not seen. Secondly, a clear band was seen at 1343 cm^{-1} , whose only viable assignment appears to be $12^1 14^1$, i.e. a combination band arising from two a_2 vibrations. We note that such a transition was seen in *pDFB*²⁹ and *pFT*⁷ from the $S_1 \leftarrow S_0$ transition, and these assignments have been confirmed by ZEKE spectroscopy for *pFT*⁷ (and in unpublished work by ourselves for *pDFB*). We were unable to identify a separate band corresponding to this transition in the REMPI spectrum unambiguously, so cannot confirm this assignment. It is plausible that the $12^1 14^1$ REMPI band could be underlying the $15^1 20^1$ band, which would suggest a value for D_{12} in the S_1 state of $(770-172 =) 598\text{ cm}^{-1}$. This is plausible as the calculated wavenumbers for the a_2 vibrations in the S_1 state were somewhat unreliable, with a “raw” calculated value of 619 cm^{-1} being in fair agreement with this derived value. An alternative value for D_{12} of 532 cm^{-1} reported in Ref. 15 (see Table 1 here) was obtained by a non-rigorous scaling of the calculated values based on wavenumbers in *pFT*. Although this appeared to work well for D_{13} and the b_1 modes, there is no prima facie reason that this should work for D_{12} . We tentatively assume there are overlapping bands in the S_1 state, and so accept the 598 cm^{-1} value for D_{12} in the S_1 state with reservations. In either case the ZEKE transition is symmetry-allowed, and the band wavenumber allows a value for D_{12} in the cation of 984 cm^{-1} to be obtained, in good agreement with the calculated value (see Table 1).

There is a $(1+1')$ accidental resonance band in the ZEKE spectrum recorded via $S_1 15^1 20^1$ at a wavenumber of 949 cm^{-1} . At this position, the “ionization” laser becomes resonant with the $S_1 28^1 \leftarrow S_0$ transition, and then the “excitation” laser ionizes this to the $11^1 28^1$ level in the cation.

ZEKE spectra of pClFB via the $9^1/29^2$ Fermi resonance bands

We now consider the close-lying pair of REMPI bands assigned to a Fermi resonance between D_9 and $2D_{29}$ in Ref. 15.

In Figure 7 we show the ZEKE spectra recorded at each of the two band maxima. In each case we see an origin band, a 11^1 band and a weak 29^1 band. A weak feature is seen at 758 cm^{-1} that

is tentatively assigned to $19^2 20^2$. The $\Delta\nu = 0$ region contains two ZEKE bands, but also present is an intense accidental resonance electron band that is coincident with the lower ZEKE band in each case. We can see from the spectra that the higher wavenumber ZEKE band of the pair is relatively more intense when exciting via the higher wavenumber REMPI band. The calculated wavenumbers, plus bands seen in other spectra, confirm the $\Delta\nu = 0$ ZEKE bands as 9^1 at 817 cm^{-1} and 29^2 at 842 cm^{-1} . Note that when exciting via the origin, the 9^1 band is very much more intense than the 29^2 band – see Figure 2(a) – and suggests that the D_9 and $2D_{29}$ levels are not in FR in the cation. Thus, we can conclude from the ZEKE spectra in Figure 7 that the REMPI band to higher wavenumber arises from an eigenstate that is dominated by $2D_{29}$. Owing to the appearance of the spectra, and by analogy with *p*FT,⁷ some mixing between these levels is expected in the S_1 state and we can thus represent the higher wavenumber transition as $29^2 \dots 9^1$, while the lower one being dominated by D_9 , is represented as $9^1 \dots 29^2$.

Moving up in wavenumber, we see a weak 7^1 ZEKE band, a band at 1196 cm^{-1} assignable to $9^1 11^1$, and the $11^1 29^2$ band being seen at 1222 cm^{-1} , but the latter is overlapped by an accidental resonance electron band, again making it difficult to be conclusive regarding the relative intensities. Overall, this behaviour appears to be consistent with the picture seen in the $\Delta\nu = 0$ region. Higher up in wavenumber, the “overtone” region is not affected by accidental resonance electron bands, and the higher wavenumber ZEKE band confirms the dominance of $2D_{29}$ character for the higher wavenumber REMPI band (indeed essentially no 9^2 band can be seen at 1642 cm^{-1}). The ZEKE spectrum recorded by the lower wavenumber REMPI feature shows clear 9^2 and $9^1 29^2$ bands, suggesting contributions from both of these levels to the S_1 eigenstates. We note that there is no obvious 29^4 band at 1688 cm^{-1} , and it seems unlikely that anharmonicity moves this band to 1671 cm^{-1} .

Various other bands are straightforward to assign. We highlight the $12^1 14^1$ combination band, seen in other spectra, and the 13^2 and 17^2 bands that appear weakly. These are each symmetry allowed and their wavenumbers are consistent with other assignments. A weak feature at 1488 cm^{-1} appears most likely to be $15^1 18^1$, which is totally symmetric, and we also see a band assignable to $10^1 18^2$, which is more intense when exciting via the lower wavenumber band.

We also see another accidental resonance feature at $\sim 1785\text{ cm}^{-1}$, at this position the “ionization” laser is resonant with the $S_1 15^2 \leftarrow S_0$ transition, and the “excitation” laser then ionizes this to

a vibrational level in the D_0^+ state, with $6^1 10^1$ being a possible assignment of this, but other levels are also close to this wavenumber.

ZEKE spectra via 6^1 , 8^1 and 10^1

When exciting via 10^1 just a single ZEKE band could be discerned on the high-wavenumber side of an accidental resonance electron band (spectrum not shown), establishing the value for D_{10} in the cation at 658 cm^{-1} .

Spectra recorded via $S_1 8^1$ and $S_1 6^1$ are shown in Figure 8. When exciting via 8^1 a clear ZEKE band is seen at 986 cm^{-1} to lower wavenumber than the first accidental resonance electron band, and the $8^1 11^1$ band can be seen clearly at 1356 cm^{-1} – see Figure 8(a). We also see a band at 1223 cm^{-1} , which we assign to $17^1 18^1$. (A possible assignment of this to $14^1 16^1$ is rejected on symmetry grounds.)

Finally, we examine the ZEKE spectrum recorded via 6^1 , which is presented in Figure 8(b). This shows a strong $\Delta v = 0$ band at 1122 cm^{-1} , confirming the value for D_6 in the cation. The other two close-lying bands to higher wavenumber are at 1138 cm^{-1} and 1175 cm^{-1} and can be assigned to $13^1 14^1$ and 7^1 . Neither of these bands can be resonantly ionized, suggesting these are simply symmetry allowed.

To higher wavenumber we see weak bands at 1364 cm^{-1} and 1435 cm^{-1} , the latter can be assigned to 17^2 . The former band can be assigned to $16^1 18^1$, but the observation of a weak band corresponding to 8^1 , means that this feature may also be expected to have a small contribution from $8^1 11^1$. There then follows a more intense set of bands, which have a contribution from one-colour accidental resonance bands on the low- and high-wavenumber sides. The ZEKE bands can be satisfactorily assigned as combinations of the intense bands in the $\Delta v = 0$ region, but each in combination with D_{11} as indicated in Figure 8(b).

ZEKE Spectra via the $10^2/5^1$ Fermi resonance

ZEKE spectra recorded via the peak positions of the two bands arising from a FR between $2D_{10}$ and D_5 are shown in Figure 9. In the low-wavenumber, $\Delta v = 0$, region of each ZEKE spectrum, two clear bands can be seen. The lower of these ZEKE bands may be associated with 10^2 , while the higher is 5^1 . In the ZEKE spectrum in Fig. 9(b), a weak peak at 1345 cm^{-1} may be seen, which has been assigned to $12^1 14^1$. It is the behaviour in the low wavenumber region that

suggests that the $2D_{10}$ and D_5 vibrations are in Fermi resonance (FR), and so we denote the lower wavenumber REMPI band as $5^1 \dots 10^2$ and the higher wavenumber one as $10^2 \dots 5^1$.

In the higher wavenumber region of Fig. 9(a), we can see the main bands in combination with D_{11} , but interestingly these are not clearly seen in the other spectrum in Fig. 9(b). In that spectrum, we see the additional band at 1763 cm^{-1} . Its width suggests this is not an accidental resonance, and the fact that it appears when exciting from one FR component and not the other indicates that this is not a FC active band. We thus looked for an accidentally overlapping transition in the $S_1 \leftarrow S_0$ step, and identified the $14^1 15^1 29^1$ transition that is expected at 1245 cm^{-1} in the S_1 state and 1766 cm^{-1} in the D_0^+ state, thus matching well. We thus conclude that the $10^2 \dots 5^1$ FR component overlaps the $14^1 15^1 29^1$ transition, giving the observed ZEKE band at 1763 cm^{-1} . The latter band arises from a totally-symmetric vibration, but does not seem to be interacting with the $2D_{10}$ nor D_5 vibrations, likely as a result of the large difference in quantum numbers.

A number of other interesting observations arise from these spectra. First, we note the intense accidental resonance band at $\sim 1940 \text{ cm}^{-1}$ in Figure 9(b). This is not present in the other spectrum, and arises as at this position, the “ionization” laser is resonant with the $S_1 6^1 \leftarrow S_0$ transition, while the “excitation” laser then ionizes to the resonant $D_0^+ 6^1 9^1$ level. We also note that the broad band at $\sim 1490 \text{ cm}^{-1}$ in Figure 9(a) is not present in the lower trace, even though the intermediate levels are in Fermi resonance. We noted that at this position, the “ionization” laser is resonant with the $S_1 17^1 20^1 \leftarrow S_0$ transition, and then the “excitation” laser could ionize to $D_0^+ 11^4$, with the width of the band attributable to excitation and ionization of both isotopologues. However, a more attractive assignment is to $11^1 30^1$ in the $S_1 \leftarrow S_0$ transition, and then $11^1 29^2 30^1$ in the cation, which we expect to have a better FCF in the ionization step; the expected isotopic shifts also seem better in line with the width of the observed band. Similarly, in the lower trace, Figure 9(b), we see a band at $\sim 1685 \text{ cm}^{-1}$, which is absent in the upper trace. We find the “ionization” laser is resonant with the $S_1 29^2 \leftarrow S_0$ transition, and then the “excitation” laser ionizes to $D_0^+ 29^4$.

Further discussion

Ionization energy shifts

In the above, we have derived the adiabatic ionization energy (AIE) of *p*ClFB as $72919 \pm 5 \text{ cm}^{-1}$. It is of interest to compare this to other related species; for example, to see whether shifts in AIEs (Δ AIEs) are additive for disubstituted species; and whether trends in Δ AIEs make chemical sense. To this end, we consider the monohalobenzenes, *p*DfB, *p*-dichlorobenzene (*p*DCIB) and *p*ClFB, together with toluene (Tol, monomethylbenzene) and *p*-xylene (*p*Xyl, *para*-dimethylbenzene). We compare the Δ AIE values (reported in Table 2) relative to benzene (Bz) and each other.

The monohalobenzenes were studied by Kwon et al.³⁰ using one-photon mass-analyzed threshold ionization (MATI) spectroscopy, and who obtained AIEs of 74229, 73177, 72570 and 70638 cm^{-1} , for fluorobenzene (FBz), chlorobenzene (ClBz), bromobenzene (BrBz) and iodobenzene (IBz), respectively. We can compare these to the AIE of Bz, which has been reported as 74555 cm^{-1} by Chewter et al.³¹, this then yields Δ AIE values for the monohalobenzenes of -326 cm^{-1} , -1378 cm^{-1} , -1985 cm^{-1} and -3917 cm^{-1} . We note that both fluorobenzene^{32,33,34} and chlorobenzene^{35,36} have been studied by other workers using ZEKE or MATI spectroscopy, with similar values having been obtained. Toluene was studied by Lu et al.³⁷ yielding an AIE of 71200 cm^{-1} , giving a Δ AIE value of -3355 cm^{-1} compared to Bz. Note that the monosubstitution stabilizes the cation relative to the neutral molecules in all cases. We can put forward an explanation for these shifts as follows. In the case of the monohalobenzenes, the halogen atom is electronegative, and so will destabilize the cationic phenyl ring via inductive effects. This destabilization will decrease with the increasing atomic number, and so decreasing electronegativity. However, there is also a mesomeric effect, whereby the lone pairs from the halogen can effectively delocalize to stabilize the positive charge in the phenyl ring. This mesomeric effect might be expected to be least for FBz and highest for iodobenzene based on electronegativities, but it is also necessary to consider orbital overlap; this leads to the electron releasing effects decreasing with increasing atomic number for the halogens. Since the overall effect is a stabilization of the cation in all cases, this suggests that the mesomeric effect dominates, with the overall (inductive+mesomeric) effect being smallest for F, and largest for I. So, although the orbital overlap is best between F orbitals and those of C, it is mitigated by the higher electronegativity of F and an approximate balance between the inductive and mesomeric effects occurs. For I, the combination of a small

mesomeric effect and also a small inductive effect, leads to a sizeable overall shift. We note that this discussion on Δ AIE values ignores zero-point vibrational energy (ZPVE) effects. The Δ ZPVE values between the S_0 and D_0^+ states are relatively small (~ 250 cm^{-1} for FBz and 146 cm^{-1} for IBz), and so these do not affect the above discussion significantly.

For Tol, the stabilization is sizeable and suggests that the explanation does not lie with the small inductive effect expected for methyl groups, but rather in terms of hyperconjugation, allowing a stabilization of the phenyl positive charge via the effective delocalization of the electrons from the methyl C-H bonds. Some comment on related trends has been made by other workers, such as recently by Shivatare et al.³⁸ and much earlier, Gounelle et al.²²

Of interest is whether Δ AIE values (see Table 2) are additive in disubstituted species or not (see Figure 10). To test this we compare the Δ AIE value derived from the AIE value obtained in our ZEKE experiments for *p*ClFB with those of FBz and ClBz. For *p*ClFB the Δ AIE value compared to Bz is -1636 cm^{-1} , while the sum of the Δ AIE values for FBz and ClBz is -1704 cm^{-1} . The agreement between the two derived values suggests that the Δ AIE values are approximately additive.

We can do a similar comparison for *p*FT, where the AIE has been reported by Ayles et al.³⁹ as 70946 cm^{-1} , giving a Δ AIE value compared to benzene of -3609 cm^{-1} . Summing the Δ AIE values from Tol and FBz, we get -3681 cm^{-1} , again showing that these are approximately additive.

Out of interest, we also look at the symmetric disubstituted species, *p*DFB, *p*DCIB and *p*Xyl. These have AIE values of 73872 cm^{-1} (Ref. 27), 72191 cm^{-1} (Ref. 40) and 68200 cm^{-1} (Ref. 9), and respective Δ AIE values compared to benzene of -683 cm^{-1} , -2364 cm^{-1} and -6355 cm^{-1} . We can compare these to twice the Δ AIE from the respective monosubstituted species that are: -652 cm^{-1} , -2756 cm^{-1} and -6710 cm^{-1} . Although the *p*DCIB values are over 10% different, the other two values are approximately additive.

In summary the Δ AIE results suggest that stabilization of the positive charge on the phenyl ring in these species is largely additive, with the perturbations caused by one substituent to another being minimal; an exception appears to be for *p*DCIB, and it would be interesting to explore the additivity further for different substituents and isomers.

Conclusions

We have confirmed the assignments of the REMPI spectrum of the $S_1 \leftarrow S_0$ transition in *p*ClFB. The ZEKE spectra allow the wavenumbers of twenty out of the thirty vibrations in the ground state of the cation to be obtained for the first time, as well as establishing a precise value for the AIE. Evidence for the presence of two Fermi resonances has been presented: $9^1 \dots 29^2$ and $5^1 \dots 10^2$. Although in many cases the $\Delta v = 0$ propensity rule appears to hold, there were several occasions where the activity suggested changes along vibrational coordinates between the S_1 state and the cation. Of interest was that the 11^1 and 14^2 bands are very close/overlapped for the two isotopologues; as such this suggests the D_{11} and $2D_{14}$ levels are not interacting. We have looked at the changes in adiabatic ionization energies and rationalized trends in terms of inductive and mesomeric electronic effects. We showed that for a number of disubstituted molecules, the Δ AIE values were approximately the sum of the shift of the corresponding monosubstituted species (within ~5%); however, there was a divergence for *p*DCIB (> 10%). It would be of interest to study such trends more widely.

Acknowledgements

We are grateful to the EPSRC for funding (grant EP/L021366/1). The EPSRC and the University of Nottingham are thanked for studentships to W.D.T., L.E.W, and D.J.K. The High Performance Computer resource at the University of Nottingham was employed for the quantum chemistry calculations.

Figure Captions

Figure 1: (a) (1+1') REMPI spectra of $p^{35}\text{ClFB}$. The ionization laser was fixed at 37990 cm^{-1} . (b) Electron signal recorded in the time-delayed ZEKE gate while scanning one of the lasers, with the other blocked. These signals arise from one-colour, two-photon accidental resonances that occur at both the one- ($S_1 \leftarrow S_0$) and two-photon ($D_0^+ \leftarrow S_1$) level.

Figure 2: (a) ZEKE spectrum of $p\text{ClFB}$ recorded via $S_1 0^0$ – see text for discussion of assignments. To higher wavenumber, we have added a section of the ZEKE spectrum (in red) that was recorded via $S_1 18^2$ (see Figure 3), which shows the position of the last one-colour accidental resonance in this region. Bands labelled with an asterisk are due to one-colour, two-photon accidental resonances – see text and trace in Figure 1(b). (b) Electron signal recorded in the time-delayed “ZEKE gate” while scanning one of the lasers, with the other blocked – see Figure 1(b) and text – shown with the two-photon wavenumber relative to the adiabatic ionization energy.

Figure 3: ZEKE spectrum of $p\text{ClFB}$ recorded via (a) 20^2 ; (b) 19^2 ; and (c) 18^2 – see text for discussion of assignments. Bands labelled with an asterisk are due to one-colour, two-photon accidental resonances – see text and trace in Figure 1(b). The bands marked with a dagger (\dagger) are two-colour accidental resonances where the “ionization” laser is resonant with an $S_1 \leftarrow S_0$ transition, and the “excitation” laser then ionizes – see text for further discussion.

Figure 4: ZEKE spectrum of $p\text{ClFB}$ recorded via (a) 30^1 , (b) 29^1 and (c) 28^1 – see text for discussion of assignments. Bands labelled with an asterisk are due to one-colour, two-photon accidental resonances – see text and trace in Figure 1(b); the bands marked with a dagger (\dagger) arise from two-colour accidental resonances where the “ionization” laser is resonant with an $S_1 \leftarrow S_0$ transition, and the “excitation” laser then ionizes – see text for further discussion.

Figure 5: ZEKE spectra of $p\text{ClFB}$ recorded via the $14^2/11^1$ bands. Upper trace: section of the REMPI spectrum showing the $14^2/11^1$ bands for each of the isotopologues, with the $19^1 20^1$ bands also labelled. The letters indicate the positions at which ZEKE spectra were recorded, and these are shown in the lower traces. See text for discussion of assignments. Bands labelled with an asterisk are due to one-colour, two-photon accidental resonances – see text and trace in Figure 1(b).

Figure 6: ZEKE spectra of *p*ClFB recorded via (a) 17^119^1 and (b) 15^120^1 – see text for discussion of assignments. Bands labelled with an asterisk are due to one-colour, two-photon accidental resonances – see text and trace in Figure 1(b). The band marked with a dagger (†) is a two-colour accidental resonance where the “ionization” laser is resonant with an $S_1 \leftarrow S_0$ transition, and the “excitation” laser then ionizes – see text for further discussion.

Figure 7: ZEKE spectra of *p*ClFB via $9^1/29^2$ Fermi resonance bands – see text for discussion of assignments. Bands labelled with an asterisk are due to one-colour, two-photon accidental resonances – see text and trace in Figure 1(b). The bands marked with a dagger (†) are two-colour accidental resonances where the “ionization” laser is resonant with an $S_1 \leftarrow S_0$ transition, and the “excitation” laser then ionizes – see text for further discussion.

Figure 8: ZEKE spectra of *p*ClFB of (a) 8^1 and (b) 6^1 – see text for discussion of assignments. Bands labelled with an asterisk are due to one-colour, two-photon accidental resonances – see text and trace in Figure 1(b).

Figure 9: ZEKE spectra of *p*ClFB via the $5^1/10^2$ Fermi resonance bands – see text for discussion of assignments. Bands labelled with an asterisk are due to one-colour, two-photon accidental resonances – see text and trace in Figure 1(b). The bands marked with a dagger (†) are two-colour accidental resonance where the “ionization” laser is resonant with an $S_1 \leftarrow S_0$ transition, and the “excitation” laser then ionizes – see text for further discussion.

Figure 10: Schematic showing the lowering of the adiabatic ionization energy (ΔAIE) compared to benzene for mono- and disubstituted benzenes, as indicated (see text for abbreviations). All values in cm^{-1} .

Table 1: Calculated and experimental vibrational wavenumbers (cm^{-1}) for the S_1 and D_0^+ states of $p\text{CIFB}$

D_i^a	S_1			D_0^+		
	Calc ^b	Expt ^c	Δ^b	Calc ^d	Expt ^e	Δ^d
a_1						
D_1	3143		0	3122		0
D_2	3130		0	3110		0
D_3	1491	1489	0	1604	1624	0
D_4	1411		0	1444		0
D_5	1211	1231	0	1305	1334	0
D_6	1037	1064	-1	1085	1122	-1
D_7	1112		0	1158	1176	0
D_8	963	962	0	965	986	0
D_9	796	793	0	804	821	0
D_{10}	617	623	-3	639	658	-3
D_{11}	348	347	-5	370	373	-5
a_2						
D_{12}	532 (619)	(598) ^f	0	976	984	0
D_{13}	482 (534)	538	0	773	782	0
D_{14}	- ^g	172	- ^g	359	358	0
b_1						
D_{15}	696 (669)	676	0	981	987	0
D_{16}	653 (606)	611	-1	855	863	0
D_{17}	558 (520)	519	0	702	718	0
D_{18}	486 (437)	431	0	497	504	0
D_{19}	254 (249)	244	0	270	277	0
D_{20}	99 (96)	94	0	99	102	-1
b_2						
D_{21}	3138		0	3121		0
D_{22}	3125		0	3111		0
D_{23}	1366		0	1400		0
D_{24}	1303		0	1458		0
D_{25}	1408		0	1295		0
D_{26}	1225		0	1245		0
D_{27}	1018		0	1100		0
D_{28}	542	546	0	573	582	0
D_{29}	394	397	0	412	421	0
D_{30}	263	265	-2	268	280	-2

^a See Ref.14. Note that a D_i label is derived by considering the vibrational motion, with the energetic ordering following that of the Mulliken procedure for $p\text{DFB}$; hence, the ordering of the D_i vibrations for other molecules, such as here, will not necessarily be in energetic order. Also note that D_5 and D_6 evolve from symmetric and asymmetric stretches in $p\text{DFB}$ into a C-F stretch (D_5) and a C-Cl stretch (D_6) – see Ref. 14 for further details and discussion.

^b TD-B3LYP/aug-cc-pVTZ calculated values for $p^{35}\text{CIFB}$ scaled by 0.97. Values in parentheses are “ $p\text{DFB}$ -scaled” values based on the calculated/experimental ratio for $p\text{DFB}$ – see Ref. 15. The Δ values are the calculated isotopic shifts between $p^{35}\text{CIFB}$ and $p^{37}\text{CIFB}$.

^c From Ref. 15.

^d UB3LYP/aug-cc-pVTZ calculated values for $p^{35}\text{CIFB}$ scaled by 0.97. The Δ values are the calculated isotopic shifts (cm^{-1}) between $p^{35}\text{CIFB}$ and $p^{37}\text{CIFB}$.

^e Present work.

^f Tentative assignment – see text.

^g The TD-B3LYP/aug-cc-pVTZ calculated value for D_{14} is unreliable – see Ref. 15 and text.

Table 2: Adiabatic ionization energy shifts for some substituted benzenes.

Molecule	$\Delta\text{AIE (actual)}^{\text{a}}/\text{cm}^{-1}$	$\Delta\text{AIE (sum)}^{\text{b}}/\text{cm}^{-1}$	%DIFF ^c
<i>p</i> FT	-3609	-3681	-2.0
<i>p</i> ClFB	-1636	-1704	-4.2
<i>p</i> DFB	-683	-652	+4.5
<i>p</i> DCIB	-2364	-2756	-16.6
<i>p</i> Xyl	-6355	-6710	+5.6

^a The experimental shift in the AIE compared to benzene.

^b Obtained from the sum of the experimental shifts of the AIEs for the corresponding monosubstituted species compared to benzene –see text.

^c $100 \times [\Delta\text{AIE}(\text{actual}) - \Delta\text{AIE}(\text{sum})] / \Delta\text{AIE}(\text{actual})$

Figure 1

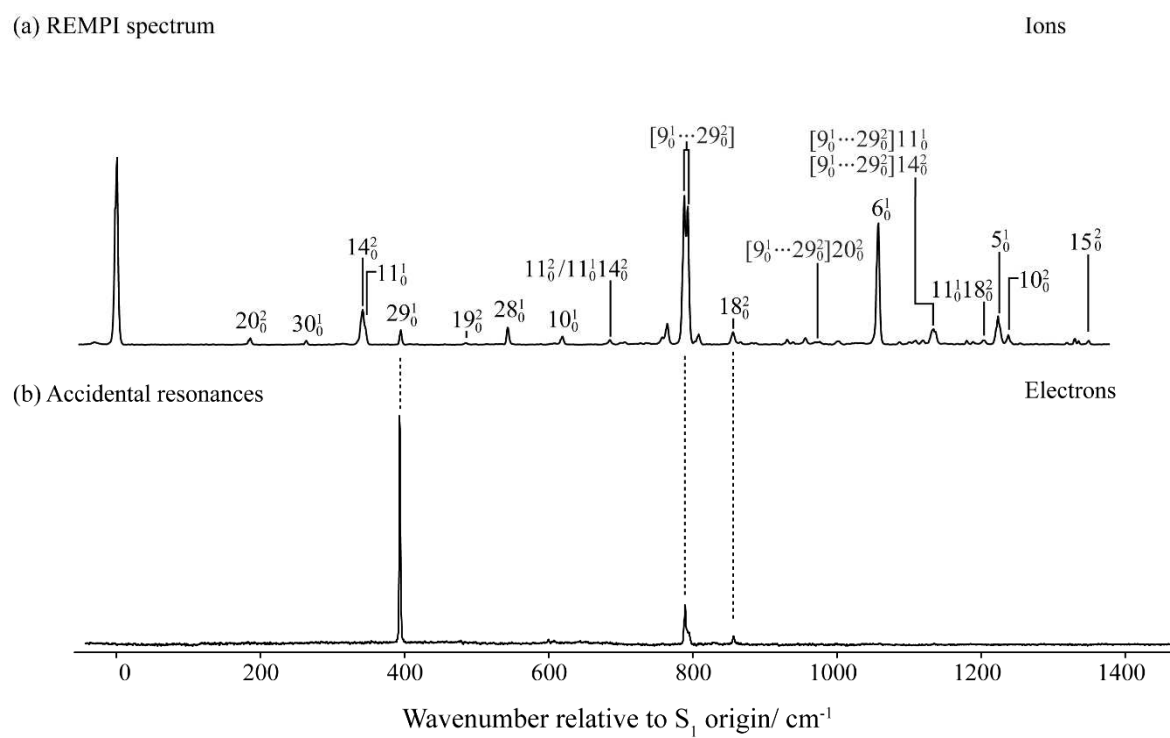


Figure 2

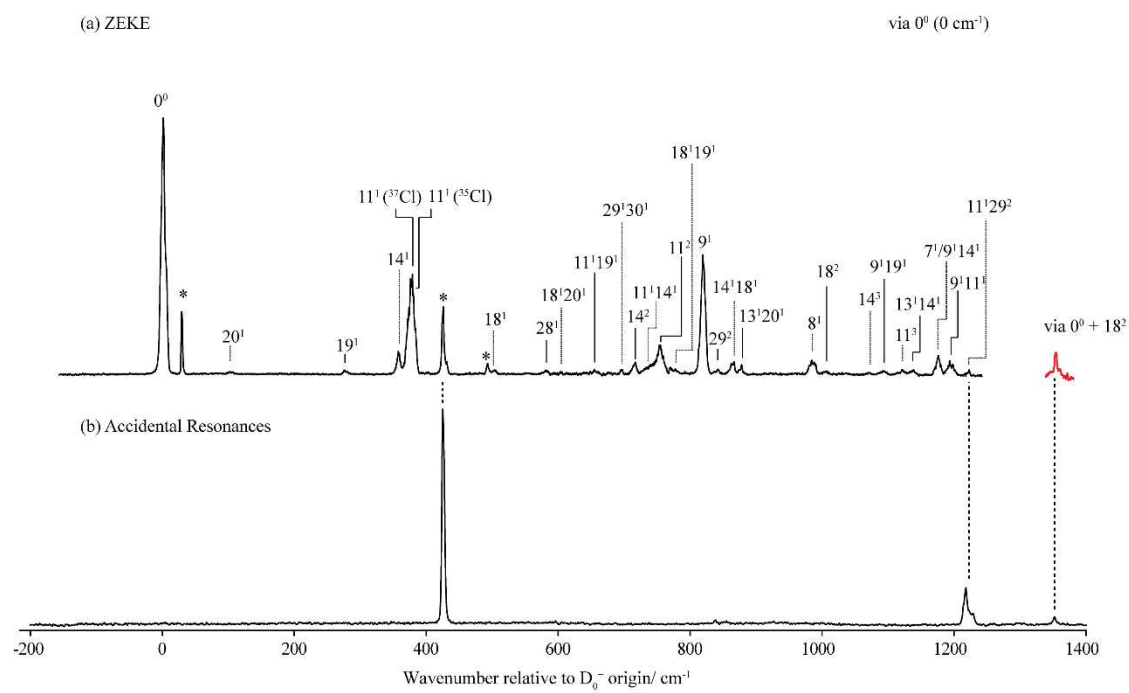


Figure 3

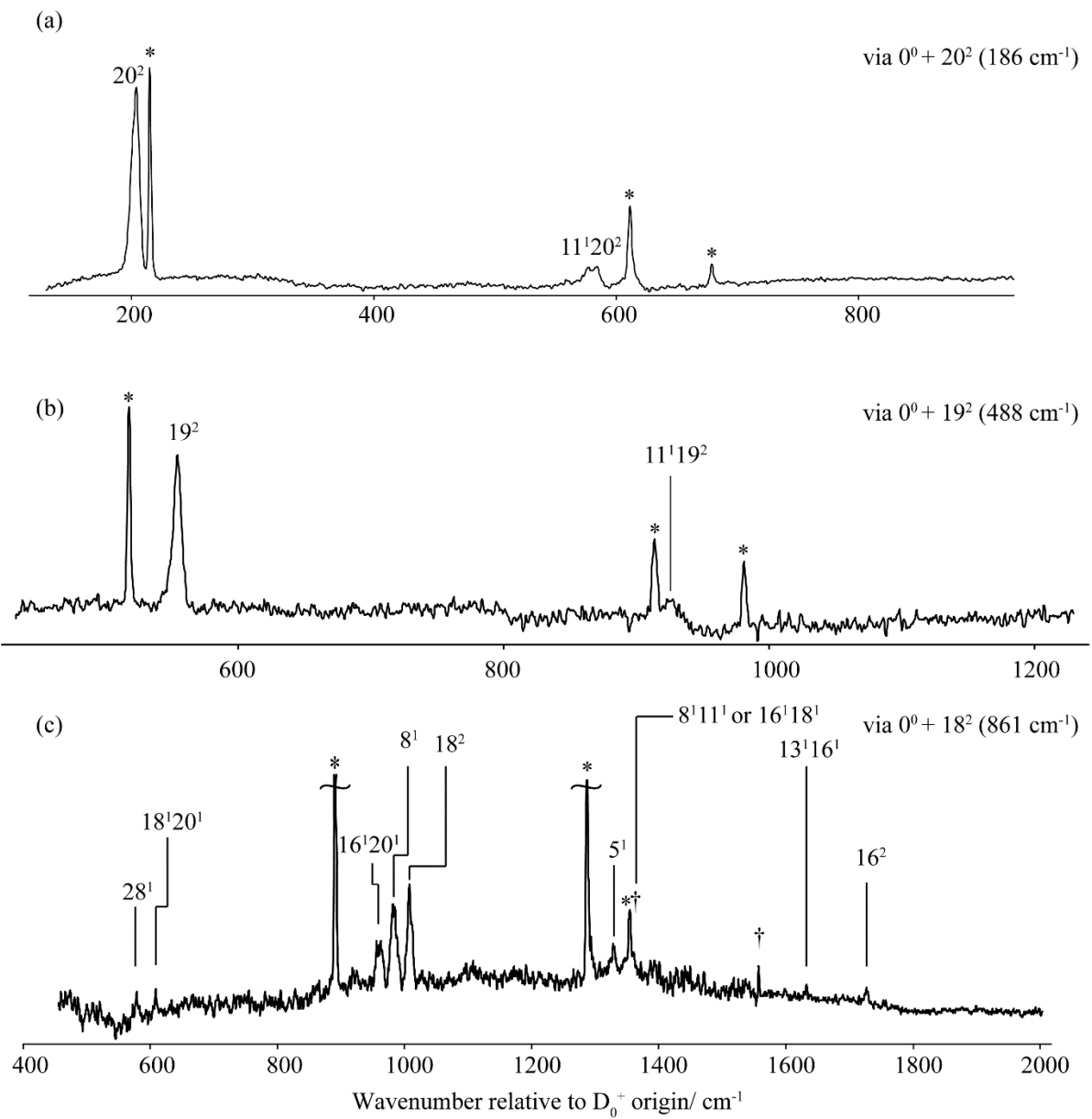


Figure 4

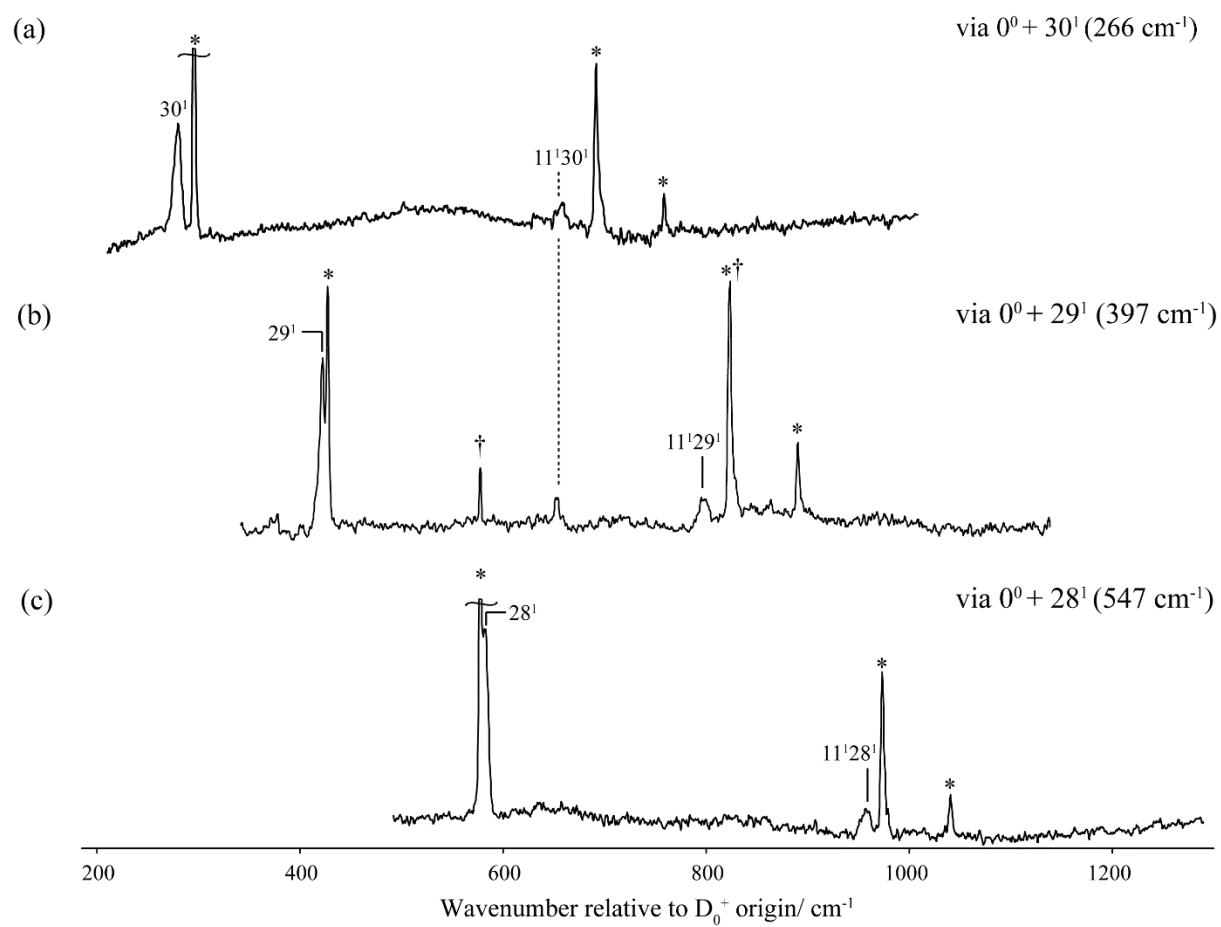


Figure 5

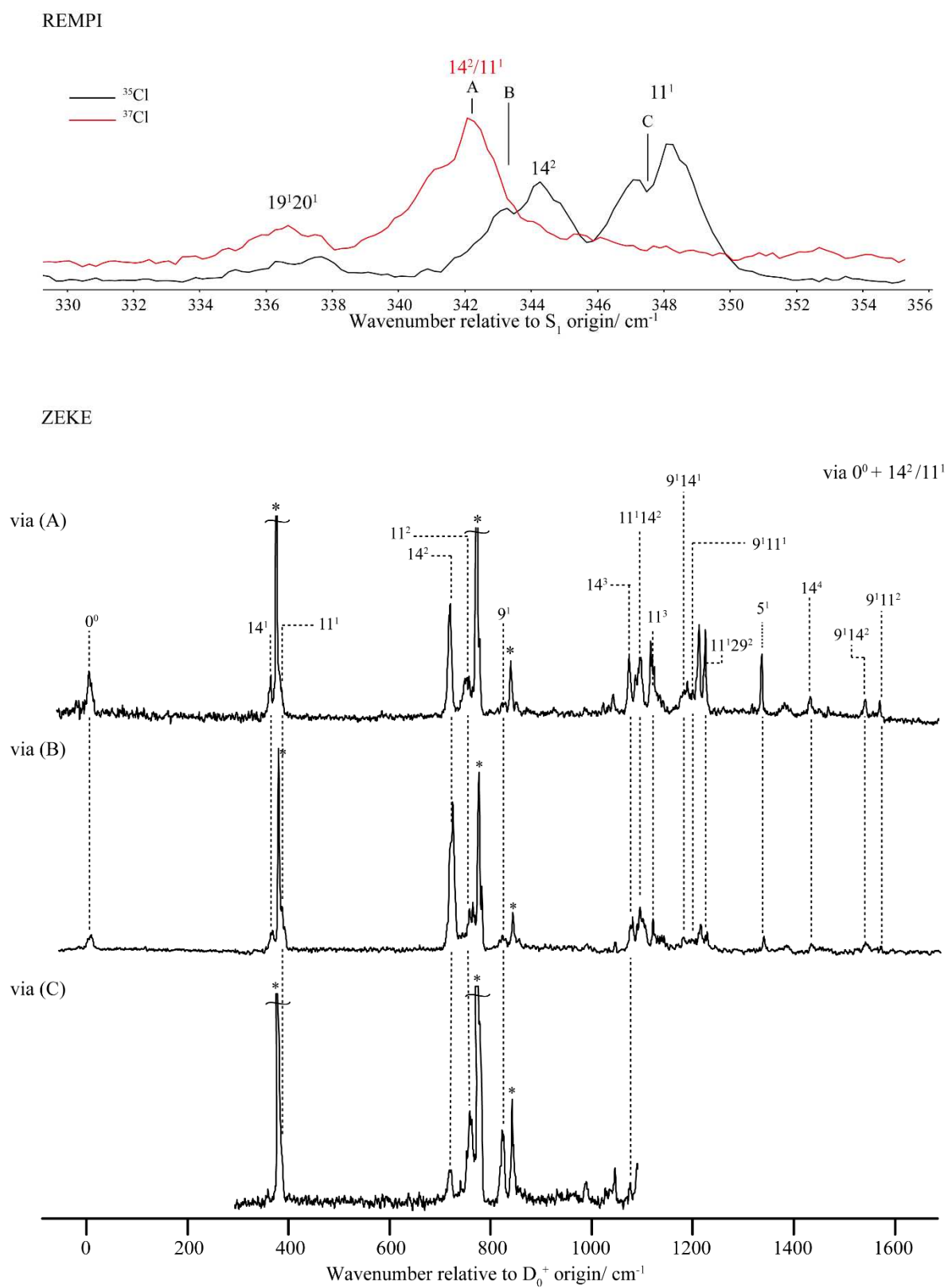


Figure 6

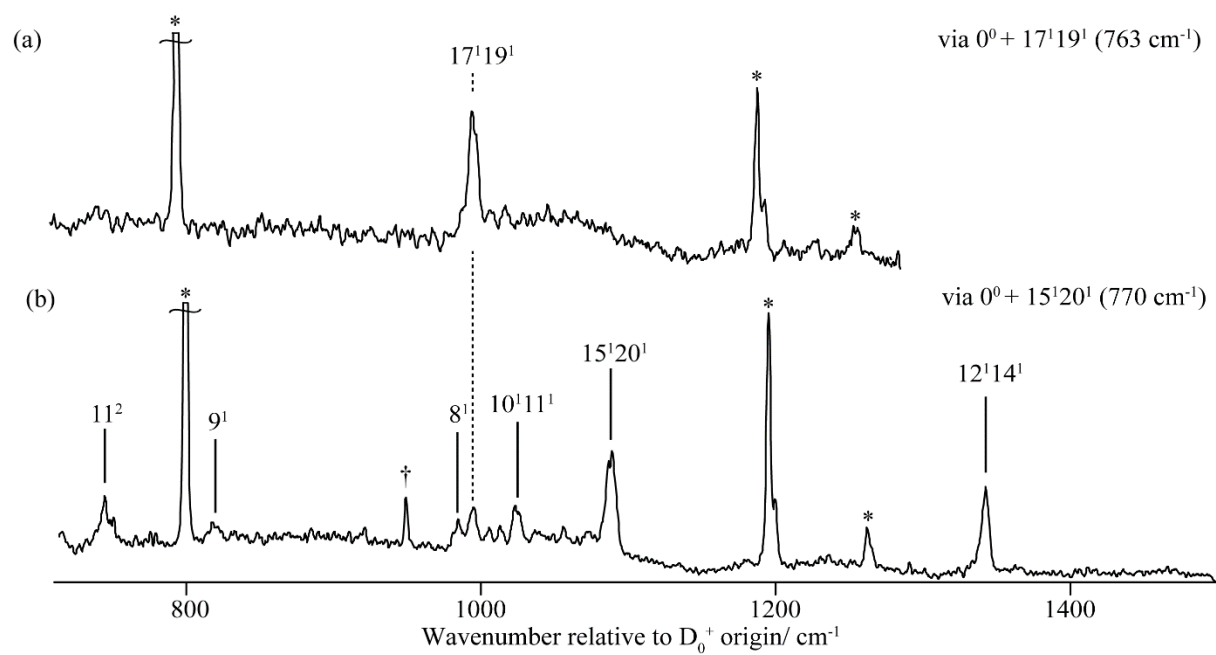


Figure 7

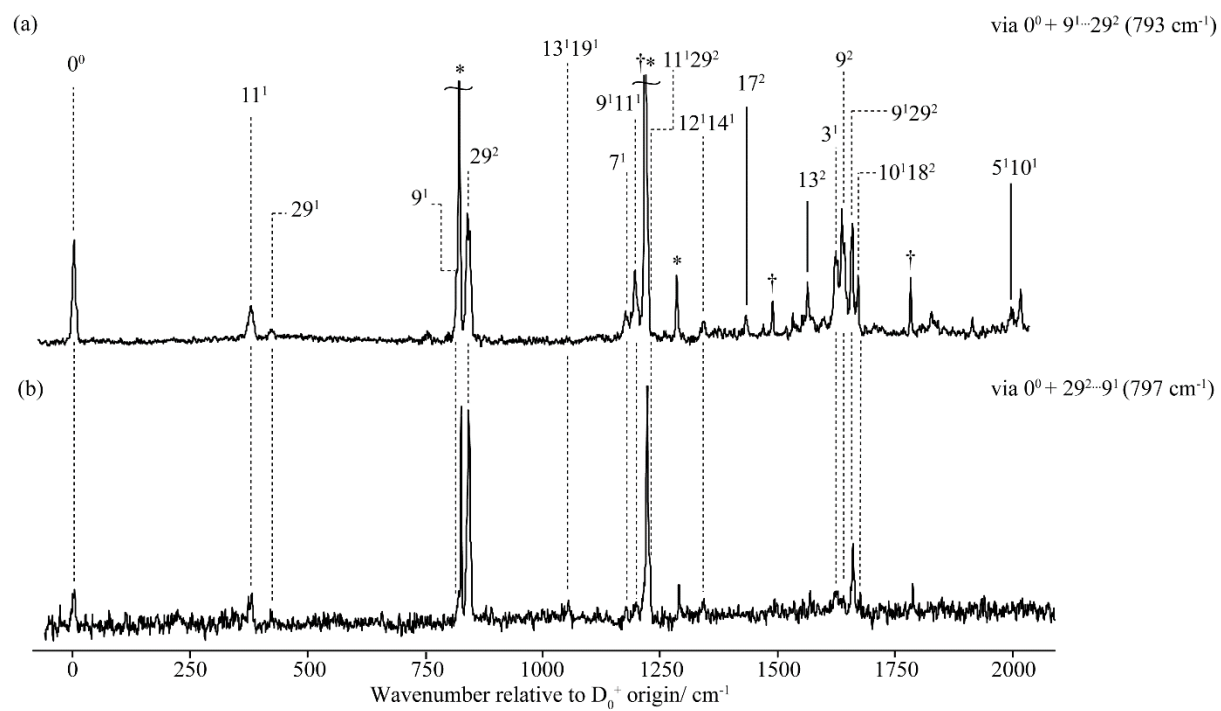


Figure 8

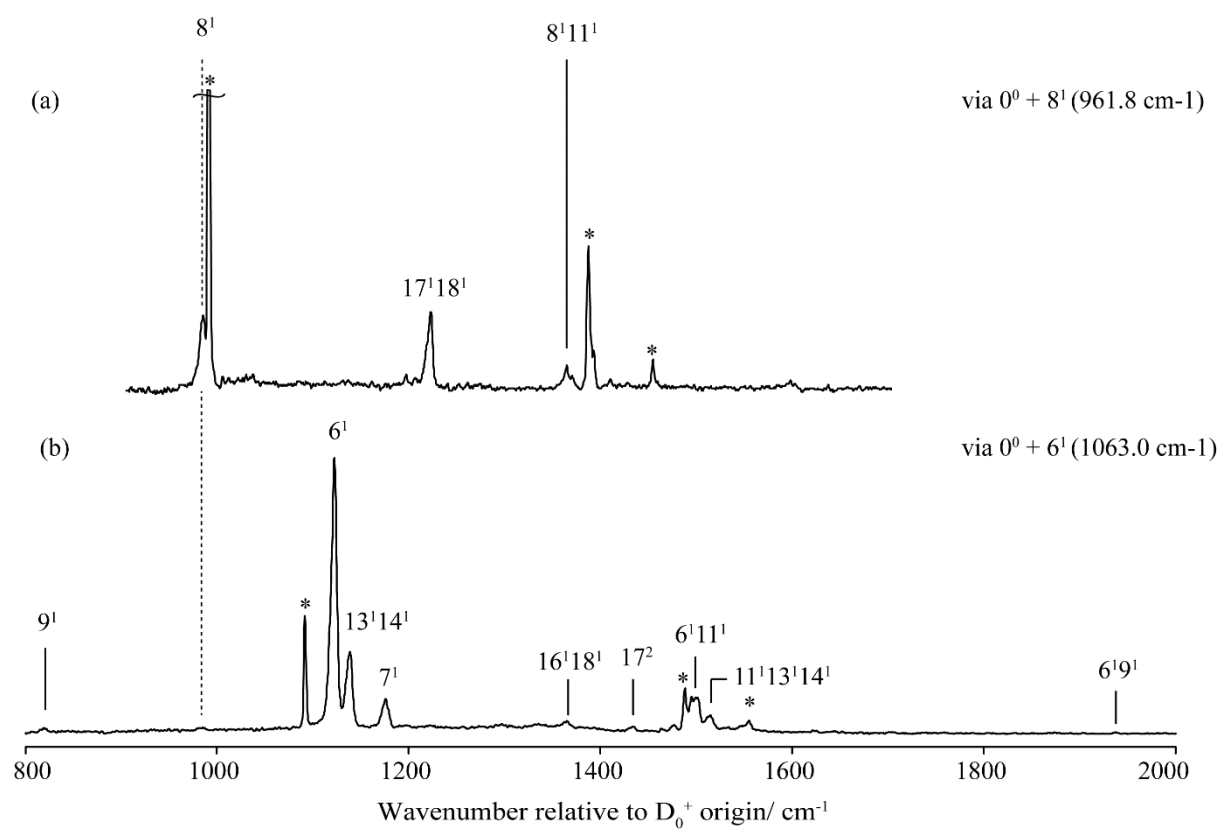


Figure 9

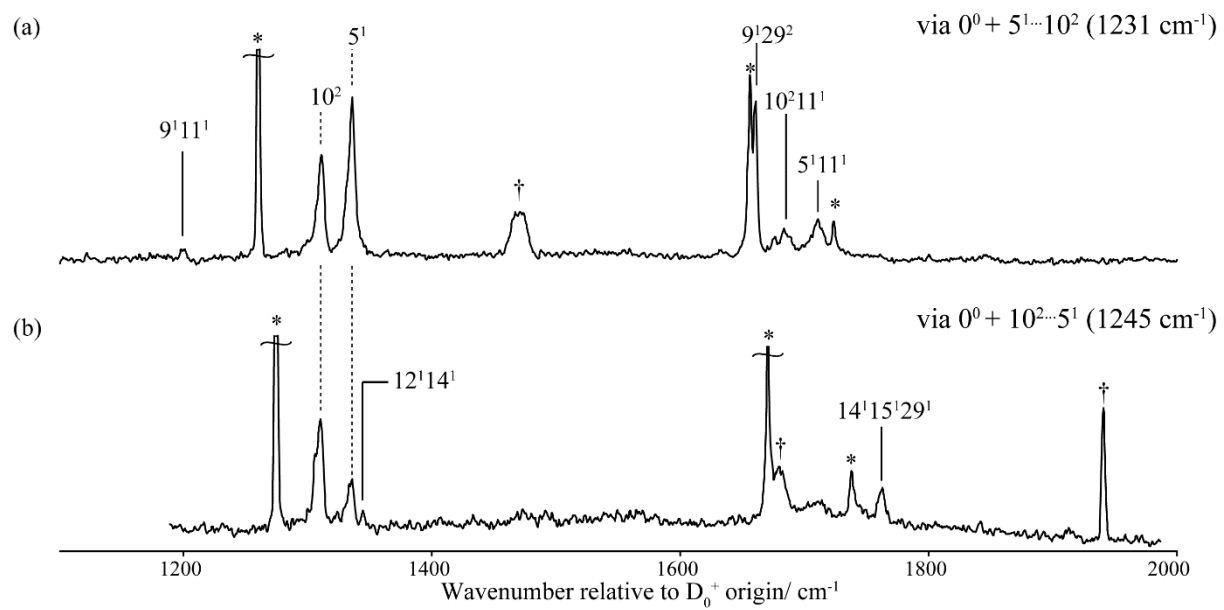
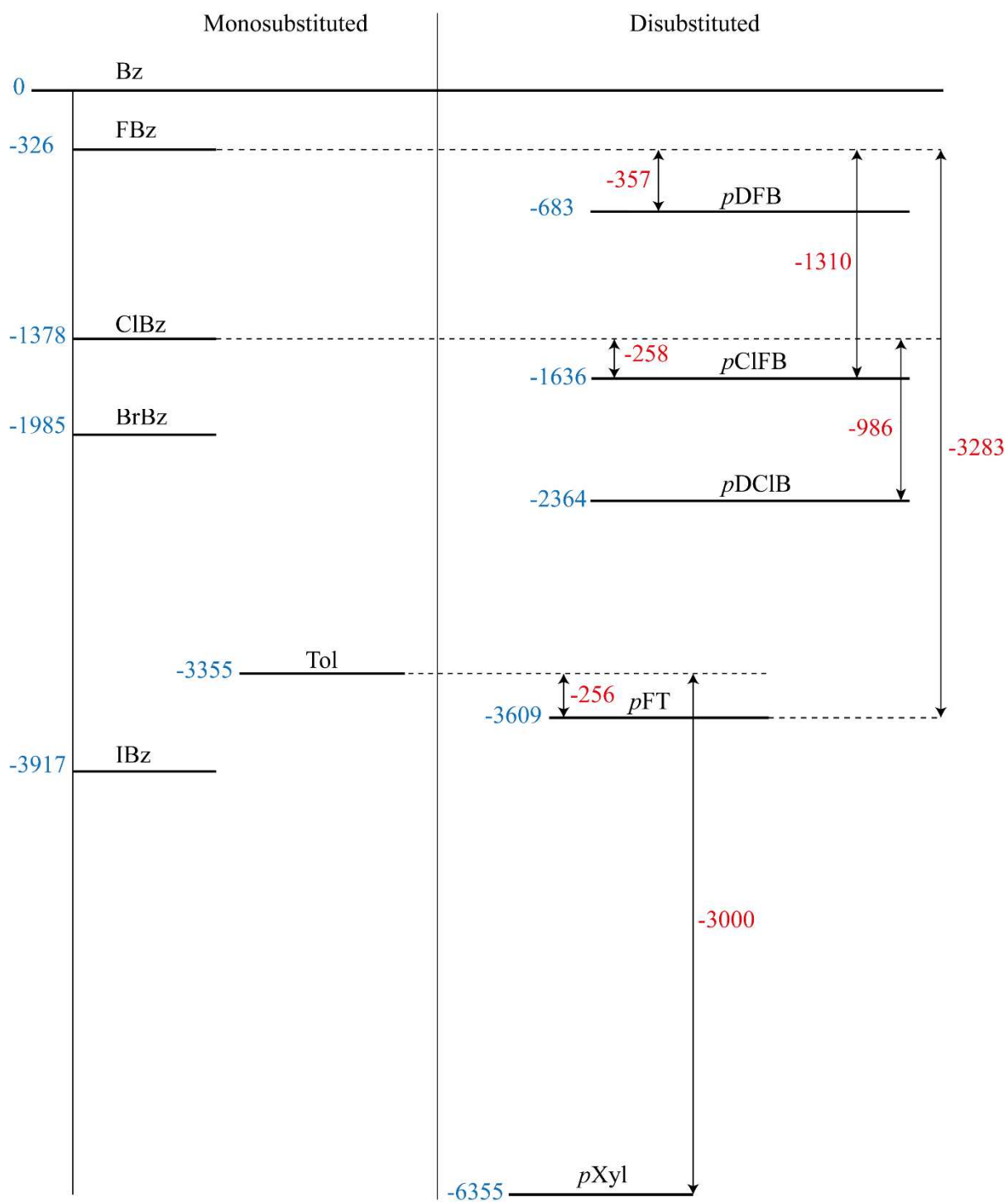


Figure 10



References

-
- ¹ J. P. Harris, A. Andrejeva, W. D. Tuttle, I. Pugliesi, C. Schriever and T. G. Wright, *J. Chem. Phys.*, 2014, **141**, 244315.
- ² A. Andrejeva, W. D. Tuttle, J. P. Harris and T. G. Wright, *J. Chem. Phys.*, 2015, **143**, 104312.
- ³ A. Andrejeva, W. D. Tuttle, J. P. Harris and T. G. Wright, *J. Chem. Phys.*, 2015, **143**, 244320.
- ⁴ A. M. Gardner, A. M. Green, V. M. Tamé-Reyes, V. H. K. Wilton and T. G. Wright, *J. Chem. Phys.*, 2013, **138**, 134303.
- ⁵ A. M. Gardner, A. M. Green, V. M. Tamé-Reyes, K. L. Reid, J. A. Davies, V. H. K. Parkes and T. G. Wright *J. Chem. Phys.*, 2014, **140**, 114038.
- ⁶ A. M. Gardner, W. D. Tuttle, L. Whalley, A. Claydon, J. H. Carter and T. G. Wright, *J. Chem. Phys.*, 2016, **145**, 124307.
- ⁷ W. D. Tuttle, A. M. Gardner, L. E. Whalley and T. G. Wright, *J. Chem. Phys.*, 2017, **146**, 244310.
- ⁸ A. M. Gardner, W. D. Tuttle, L. E. Whalley and T. G. Wright, *Chem. Sci.*, 2018, **9**, 2270.
- ⁹ W. D. Tuttle, A. M. Gardner, K. B. O'Regan, W. Malewicz and T. G. Wright, *J. Chem. Phys.*, 2017, **146**, 124309.
- ¹⁰ A. M. Gardner, W. D. Tuttle, P. Groner and T. G. Wright, *J. Chem. Phys.*, 2017, **146**, 124308.
- ¹¹ A. M. Gardner and T. G. Wright, *J. Chem. Phys.*, 2011, **135**, 114305.
- ¹² W. D. Tuttle, A. M. Gardner, A. Andrejeva, D. J. Kemp, J. C. A. Wakefield and T. G. Wright, *J. Molec. Spectrosc.*, 2018, **344**, 46.
- ¹³ D. J. Kemp, W. D. Tuttle, F. M. S. Jones, A. M. Gardner, A. Andrejeva, J. C. A. Wakefield and T. G. Wright, *J. Molec. Spectrosc.*, 2018, **346**, 46.
- ¹⁴ A. Andrejeva, A. M. Gardner, W. D. Tuttle and T. G. Wright, *J. Molec. Spectrosc.*, 2016, **321**, 28.
- ¹⁵ W. D. Tuttle, A. M. Gardner and T. G. Wright, *Chem. Phys. Lett.*, 2017, **684**, 339.
- ¹⁶ N. A. Narasimham, M. Z. El-Sabban and J. R. Nielsen, *J. Chem. Phys.*, 1956, **24**, 420.
- ¹⁷ J. H. S. Green, *Spectrochim. Acta*, 1970, **26A**, 1503.
- ¹⁸ T. Cvitaš and J. M. Hollas, *Molec. Phys.*, 1970, **18**, 261.
- ¹⁹ Y. Numata, Y. Ishii, M. Watahiki, I. Suzuka and M. Ito, *J. Phys. Chem.*, 1993, **97**, 4930.
- ²⁰ C. Riehn, K. Buchhold, B. Reimann, S. Dafari, H.-D. Barth, B. Brutschy, P. Tarakeshwar and K. S. Kim, *J. Chem. Phys.*, 2000, **112**, 1170.
- ²¹ A. D. Baker, D. P. May and D. W. Turner, *J. Chem. Soc. B*, 1968, 22.

-
- ²² Y. Gounelle, J. Jullien, D. Solgadi, R. Botter and F. Menes, *J. Chim. Phys.*, 1975, **10**, 1094.
- ²³ M. Mohraz, J. P. Maier, E. Heilbronner, G. Bieri and R. H. Shiley, *J. Elec. Spect. Rel. Phenom.*, 1980, **19**, 429.
- ²⁴ J. P. Maier, O. Marthaler, M. Mohraz and R. H. Shiley, *Chem. Phys.*, 1980, **47**, 295.
- ²⁵ S. G. Lias and P. J. Ausloos, *J. Am. Chem. Soc.*, 1978, **100**, 6027.
- ²⁶ Gaussian 09, Revision E.01, M. J. Frisch *et al.* Gaussian, Inc., Wallingford CT, 2016.
- ²⁷ D. Rieger, G. Reiser, K. Müller-Dethlefs and E. W. Schlag, *J. Phys. Chem.*, 1992, **96**, 12.
- ²⁸ G. Reiser, D. Rieger, T. G. Wright, K. Müller-Dethlefs and E. W. Schlag, *J. Phys. Chem.*, 1993, **97**, 4335.
- ²⁹ A. E. W. Knight and S. H. Kable, *J. Chem. Phys.*, 1988, **89**, 7139.
- ³⁰ C. H. Kwon, H. L. Kim and M. S. Kim, *J. Chem. Phys.*, 2002, **116**, 10361.
- ³¹ L. A. Chewter, M. Sander, K. Müller-Dethlefs and E. W. Schlag, *J. Chem. Phys.*, 1987, **86**, 4737.
- ³² G. Lembach and B. Brutschy, *J. Phys. Chem.*, 1996, **100**, 19758.
- ³³ H. Shinohara, S. Sato and K. Kimura, *J. Phys. Chem. A*, 1997, **101**, 6736.
- ³⁴ I. Pugliesi, N. M. Tonge and M. C. R. Cockett, *J. Chem. Phys.*, 2008, **129**, 104303.
- ³⁵ T. G. Wright, S. I. Panov and T. A. Miller, *J. Chem. Phys.*, 1995, **102**, 4793.
- ³⁶ G. Lembach and B. Brutschy, *Chem. Phys. Lett.*, 1997, **273**, 421.
- ³⁷ K.-T. Lu, G. C. Eiden and J. C. Weisshaar, *J. Phys. Chem.*, 1992, **96**, 9742.
- ³⁸ V. S. Shivatare, A. Kundu, G. N. Patwari and W. B. Tzeng, *J. Phys. Chem. A*, 2014, **118**, 8277.
- ³⁹ V. L. Ayles, C. J. Hammond, D. E. Bergeron, O. J. Richards and T. G. Wright, *J. Chem. Phys.*, 2007, **126**, 244304.
- ⁴⁰ A. Gaber, M. Riese and J. Grotemeyer, *J. Phys. Chem. A*, 2008, **112**, 425. (Note that the AIEs for the three different dichlorobenzenes are not cited in the correct order in the Abstract of this work – see the main text of that article.)